JOURNAL OF GEOPHYSICAL RESEARCH, VOL. 102, NO. A1, PAGES 285–294, JANUARY 1, 1997

An updated model of the hot nitrogen atom kinetics and thermospheric nitric oxide

J.-C. Gérard
Laboratoire de Physique Atmosphérique et Planétaire, Institut d'Astrophysique, Université de Liège, Liège, Belgium

D. V. Bisikalo and V. I. Shematovich
Institute of Astronomy of the Academy of Sciences, Moscow

J.W. Duff
Spectral Sciences, Inc., Burlington, Massachusetts

Abstract. New observations and reanalysis of previous measurements suggest an upward revision of the measured thermospheric nitric oxide density. Our previous model of NO production by fast $N(^4S)$ atom collisions with O_2 has been updated. It includes the effect of soft solar X rays, Auger electrons, and a detailed treatment of N_2 dissociative ionization channels. In addition, new calculations indicate that the transfer of translational energy in $N + N_2$ collisions is less efficient than in the hard sphere approximation. This result leads to reevaluation of the energy dependent relaxation cross section and to an upward revision of the reacting efficiency of collisions of N with O_2 to form nitric oxide. The calculated peak NO density increases by a factor of ~ 2 when the effect of superthermal nitrogen atoms is included. The model response of the $N(^4S)$ energy distribution function and NO density to solar cycle variations is presented. The NO density at 110 km changes from 5.4×10^7 to 1.3×10^8 cm^{-3} when the solar $F_{10.7}$ index varies from 70 to 245, but its response depends on the magnitude of the soft X ray increase with solar activity.

1. Introduction

Reaction of nonthermal ground state $N(^4S)$ atoms with O_2 was suggested as a possible source of nitric oxide molecules in the atmosphere [*Solomon,* 1983]. Hot nitrogen atoms are produced by exothermic photochemical processes in the thermosphere so that, at steady state, their distribution function departs substantially from Maxwellian at energies above $\sim$ 0.3 eV [*Shematovich et al.,* 1991, 1992]. These superthermal atoms react with O_2 to form NO at an energy dependent rate considerably faster than at thermal equilibrium for gas temperatures encountered in the thermosphere [*Duff et al.,* 1994]. *Gérard et al.* [1991, 1995] demonstrated that this process is, indeed, an additional source of thermospheric nitric oxide in the sunlit atmosphere. The dependence of the efficiency of the fast N source of NO on solar activity was discussed by *Gérard et al.* [1993]. Several recent studies [*Barth et al.,* 1988; *Siskind et al.,* 1990, 1995; *Gérard et al.,* 1995] have also pointed out the critical role played in the lower thermosphere by solar soft X rays as a source of N_2 ionization and dissociation, leading to the production of atomic nitrogen in the $N(^4S)$ ground state and metastable $N(^2D)$ state, both precursors of the formation of nitric oxide by reaction with O_2. Unfortunately, large uncertainties exist about the solar cycle dependence of the soft X ray flux ($\lambda < 100$ Å) [*Tobiska,* 1991; *Siskind et al.,* 1995]. Ionization of N_2 by this part of the solar spectrum produces energetic photoelectrons which, in turn, produce further ionization and dissociation. In particular, N_2 ionization by solar radiation at wavelength less than 31 Å eject Auger photoelectrons with energy about 360 eV.

Recent observations of nitric oxide column density [*Clancy et al.,* 1992] and number density maximum at 110 km [*Siskind et al.,* 1995, *Barth et al.,* 1996] and new correction factors introduced to account for self-absorption effects in satellite NO measurements by resonance scattering [*Eparvier and Barth,* 1992] have lead to an upward revision of previously estimated NO peak densities. These new data suggest a need to revise the NO photochemistry and reevaluate the role of fast N and energetic photoelectrons as a source of thermal and nonthermal nitrogen atoms.

Copyright 1997 by the American Geophysical Union.

Paper number 96JA02868.
0148-0227/97/96JA-02868$09.00

New features have been added to the kinetic model which is used to calculate the energy distribution function of fast $N(^4S)$ atoms: (1) Additional sources of hot $N(^4S)$ atoms have been included. The contribution of fast $N(^4S)$ atoms created by dissociative ionization of N_2 by XUV solar photons and high-energy photoelectrons has been considered. The energy distribution of the nascent $N(^4S)$ atoms is calculated using available laboratory data. (2) The broadening of the energy distribution function of the nascent fast N atoms produced by exothermic processes has been considered. (3) Finally, and more importantly, new information has recently become available concerning the efficiency of the reaction of superthermal $N_f(^4S)$ reaction with O_2 to form NO and its competitive thermalization process, that is, nonreactive (elastic and inelastic) collisions with ambient molecules. These calculations indicate that the reactive fraction of fast $N(^4S)$ atoms is significantly larger than used in previous versions of this model and leads to an upward revision of the $N_f(^4S) + O_2$ source of nitric oxide.

In addition, revisions of the photochemical code based on the work of *Siskind et al.*[1995] have been made. They include (1) the extension of the solar soft X ray flux down to 11 Å, (2) the consideration of the production of energetic Auger electrons by photoionization of N_2, O_2, and O and by fast photoelectron impact, and (3) the detailed treatment of the various energetic channels in the dissociative ionization of N_2. Photoelectrons produced in this process may carry up to 800 eV kinetic energy.

In this study, we describe updates made recently to the photochemical (section 2.1) and new features of the fast N kinetic model (section 2.2) incorporating new processes or revised cross sections. In particular, we present a new calculation of the relaxation cross section of fast N atoms in N_2 and its implication in the reaction efficiency of $N_f(^4S)$ with O_2 (section 2.3). Section 4 discusses the results of the new nitrogen atom distribution function and its impact on the NO density at low and high solar activity levels.

2. Hot $N(^4S)$ Photochemistry and Kinetics Models and Their Updates

The model calculations were made using the following procedure:

1.) The detailed processes of XUV and soft X ray absorption and the subsequent kinetics of fast photoelectrons are calculated using the kinetic model described by *Shematovich et al.* [1991, 1992]. This model includes excitation, dissociation, and direct, dissociative and Auger ionization processes induced by the photon and electron fluxes. For the photoelectron flux calculations, we use an energy grid extending from thermal energies up to 1000 eV, and we consider energy deposition of the cascade electrons.

2.) The output of the previous step, including the frequencies of XUV and soft X ray photon and fast photoelectron impact processes on the thermospheric gases is used by the one-dimensional chemical-diffusive odd nitrogen model [*Gérard and Taieb*, 1986; *Gérard et al.*, 1991]. Vertical steady state profiles of the odd nitrogen constituents are calculated by this code. They are hereafter referred to as the standard case (no hot $N(^4S)$ contribution).

3.) Production rates and initial kinetic energy distribution functions of hot $N(^4S)$ are calculated in steps a and b by appropriate codes: i at step a for N_2 dissociation and dissociative ionization by photons and photoelectrons; ii at step b for exothermic chemical reactions (3). These values are provided to the hot $N(^4S)$ kinetics code [*Shematovich et al.*, 1991, 1992] which calculates the relaxation of hot atoms by elastic collisions with the ambient atmospheric gases and by reactive collisions with O_2. This kinetic model provides the steady state energy distribution functions of $N(^4S)$ at different altitudes and the height dependent fraction of hot $N(^4S)$ reacting with O_2 (reaction efficiency).

4.) Using the reaction efficiency and the total production rate of hot $N(^4S)$, the odd nitrogen species profiles are calculated by the photochemical code. These profiles show the influence of hot $N(^4S)$ on the NO concentration in the lower thermosphere. These profiles are referred to hereafter as hot N cases.

2.1. Photochemical Model

The hot $N(^4S)$ photochemistry in the lower thermosphere is driven by the solar EUV flux in the different wavelength intervals (soft X rays below the 50 Å, XUV below 250 Å, and EUV below 1100 Å). Fast photoelectrons (with energies less than 1000 eV) formed by photoionization of N_2 also play a significant role in the ionization and dissociation of N_2. In comparison to our previous studies [*Gérard et al.*, 1993, 1995], we have extended the soft X ray flux down to 11 Å using the experimental data by *Donnally and Pope* [1973]. The suggestion that this wavelength range can play a role in the odd nitrogen photochemistry was made by *Siskind et al.* [1995]. This extension leads to additional sources of hot $N(^4S)$ atoms and high energy electrons produced by N_2 dissociative ionization and Auger ionization processes:

$$N_2 + h\nu \quad \text{(soft X ray)} \rightarrow \begin{cases} N_2^+ + e_\nu \\ (N_2^+)^* + e_\nu \rightarrow N_2^{++} + e_{\text{Aug}} + e_\nu \\ N^+ + N(^4S) + e_\nu \end{cases} \quad (1)$$

$$N_2 + e_\nu \quad (E < 1000\,\text{eV}) \rightarrow \begin{cases} N_2^+ + e'_\nu + e \\ (N_2^+)^* + e'_\nu + e \rightarrow N_2^{++} + e'_\nu + e + e_{\text{Aug}} \\ N^+ + N(^4S, {}^2D, {}^2P) + e'_\nu + e \end{cases} \quad (2)$$

The updated model also includes the Auger ionization of atomic and molecular oxygen. The consideration of K-shell ionization [*Moddeman et al.*, 1971] leads to the formation of high-energy Auger electrons in ad-

dition to the secondary photoelectron. Consequently, the electron impact dissociation and ionization rates of N_2 increase in the lower thermosphere, leading to additional production of odd nitrogen.

The partial cross sections for N_2, O_2, and O for solar flux down to 18 Å were adopted from *Conway* [1989] and are very close to those published by *Richards et al.* [1994]. For the 11–17 Å interval, values from *Siskind et al.* [1995] were adopted. Other cross sections for photon and electron impact and chemical rate coefficients are identical to the previous versions of the model [*Shematovich et al.*, 1991, 1992]. In particular, the branching ratio of the $N(^2D)$ production by electron impact dissociation of N_2 and by chemical processes are the same as in the work of *Gérard et al.* [1993, 1995]. As previously, the rate coefficient for $N(^2D)$ quenching by atomic oxygen is 6.7×10^{-13} cm^{-3} s^{-1}, the most recent laboratory determination of this important quantity [*Fell et al.*, 1990]. Molecular and eddy vertical transport are considered for NO and $N(^4S)$ as described by *Gérard and Taieb* [1986], and photochemical equilibrium is assumed for $N(^2D)$, ions, and electrons.

2.2. Hot $N(^4S)$ Kinetics Model

Theoretical studies [*Whipple*, 1974; *Sharma et al.*, 1996] of the kinetics of bimolecular chemical reactions indicate that the products of exothermic reactions have energy distributions different from the thermal ones. This fact leads to additional broadening of the initial energy distribution functions of the reaction products [*Sharma et al.*, 1996] and, consequently, can influence the kinetics of the reaction products. This effect was not considered in our previous studies. In this work, this additional broadening is taken into consideration in the calculation of the $N(^4S)$ energy distribution function (EDF). The analytical solution for the initial EDF of the reaction products is known only for a few simple cases when the reaction cross sections are independent of energy. In the revised model, we consider four main exothermic chemical sources of $N_f(^4S)$:

$$\begin{array}{lcll} NO^+ + e & \rightarrow & N(^4S) + O & +2.75\text{eV} \\ O^+ + N_2 & \rightarrow & NO^+ + N(^4S) & +1.09\text{eV} \\ N^+ + O_2 & \rightarrow & O_2^+ + N(^4S) & +1.72\text{eV} \\ N(^2D) + O & \rightarrow & O + N(^4S) & +2.38\text{eV} \end{array} \quad (3)$$

All these sources have strongly energy dependent cross sections [*Rees*, 1989]. A numerical Monte Carlo model was developed to calculate the initial energy distribution functions of the hot $N(^4S)$ atoms. This code provides the initial hot $N(^4S)$ distribution function for given cross sections and exothermic reaction energy releases. In our previous studies, only direct photon and electron impact dissociation of N_2 was considered as the main direct source of hot $N(^4S)$ atoms. In this work, we also consider additional production of hot $N(^4S)$ by dissociative ionization of N_2 by XUV photons and by high energy electrons. The energy distributions of $N(^4S)$ produced by photons are derived from the experimental studies by *Gardner and Samson* [1975]. The EDF of $N(^4S)$ produced by electron impact was adopted from *Locht et al.* [1992] and *Van Zyl and Stephen* [1994].

The influence of hot $N(^4S)$ on the odd nitrogen photochemistry strongly depends on the rates of two processes: (1) the reaction of hot nitrogen with O_2 to produce NO, and (2) the cooling of the hot particles in relaxation (elastic and inelastic) collisions with the ambient gases (N_2, O_2, and O). In this model, we use the energy dependent cross section for reaction of hot $N(^4S)$ with O_2 by *Polak et al.* [1984], which is consistent with recent results by *Duff et al.* [1994]. The situation concerning the total relaxation sections is more complex. In previous studies, we used gasdynamical estimates of the elastic cross sections deduced from the consideration of diffusive processes. The possibility that the cross sections are smaller for high-energy collisions was considered by decreasing its value by an arbitrary factor. In this work, we present new calculations of the relaxation cross section of $N(^4S)$ in N_2 and apply these new energy dependent values to the calculation of the $N(^4S)$ energy distribution.

2.3. Energy Dependent $N(^4S)$ Relaxation Cross Sections

The most uncertain quantity in predicting the contribution of fast $N(^4S)$ atoms to NO formation is the cross section for relaxation of the translationally hot atoms by collisions with the ambient atmosphere. Although there are several theoretical examples of the relaxation of fast atoms in atomic collisions [*Yee and Dalgarno*, 1985; *Tharamel et al.*, 1995], little is known about the relaxation of fast atoms in molecular collisions (i.e., where internal degrees of freedom of the colliding partner may be important). Previous estimates of relaxation cross sections for $N+N_2$ based on diffusion coefficients [*Morgan and Schiff*, 1964] have ranged from 10 Å^2 to 35 Å^2 [*Shematovich et al.*, 1991, 1992]. In order to assess the effect of internal degrees of freedom and provide a better description of the relaxation of fast $N(^4S)$ atoms by molecular N_2, the quasi-classical trajectory (QCT) method [*Truhlar and Muckerman*, 1979] is used to compute the translational energy dependence of the energy transfer cross sections and the final N_2 vibrational/rotational state distributions. The interaction energy for the $N+N_2$ collisions is represented by a London-Erying-Polanyi-Sato semiempirical potential energy surface with parameters chosen such that the barrier to reaction is approximately correct [*Laganà et al.*, 1987]. Although the accuracy of the potential energy surface for energy transfer calculations is currently unknown, the results should provide a semiquantitative description of the relaxation process. The final vibrational and rotational distributions are obtained using the standard histogram method as modified by *LaBudde and Bernstein* [1973] for symmetrical diatomic molecules. Calculations by *Pattengill* [1975] on the $Ar+N_2$ system have shown that method I of Labudde and Bernstein is to be preferred for treating rotational

energy transfer. For the present study, the dominant inelastic process is translational to rotational (T → R) energy transfer. Numerous studies on rotational energy transfer in atom-molecule collisions have established the validity of classical mechanics for calculating energy transfer cross sections [*LaBudde and Bernstein,* 1973; *Pattengill,* 1975]. Standard Monte Carlo techniques are used to compute the energy transfer cross sections as a function of the initial translational energy E_T and the initial N_2 vibrational-rotational states which are selected from a 500 K Boltzmann distribution.

The differential translational energy transfer cross section $d\sigma_T/dE_{T'}$, which describes the cross section for atoms with initial translational energy E_T collisionally relaxing to a final translational energy $E_{T'}$, is a well defined classical quantity for $E_{T'} \neq E_T$. At $E_{T'} = E_T$ there is a nonintegrable singularity, which prohibits a purely classical calculation of the translational energy transfer cross section because of the large impact parameter contribution to the elastic scattering cross sectio σ_{el}. However, the influence of large impact parameter scattering on the total cross section can be estimated by calculating the total cross section for N+N_2 using the Massey-Mohr formula [*Massey and Mohr, 1934; Bernstein et al.,* 1963] including the Landau-Lifshitz correction factor. The parameters for the attractive long-range interaction, which is the dominant factor in determining the total cross section, are calculated from well-known formulas for dispersion forces [*Hirschfelder et al.,* 1954]. In summary, the energy transfer cross section for $E_{T'} = E_T$ is estimated from the long-range interaction using the Massey-Mohr equation, while the QCT method is used for $E_{T'} \neq E_T$.

The results of relaxation calculations are summarized in Table 1 for a range of initial translational energies (in the laboratory coordinate system) from 0.075 to 3 eV. Although the inelastic T → R cross section σ_{in} only comprises approximately 1/8 to 1/4 of the total cross section (see Table 1), Figure 1 indicates that inelastic processes are the dominant mechanism for N(^4S) relaxation. Elastic scattering is ineffective in N(^4S) relaxation, making an important contribution only for $E_{T'} \neq E_T$ (large impact parameter processes). The efficiency of transferring translation energy is illustrated by considering the average fraction of translational energy transferred per collision Δf_T, which is approximately 5% as shown in Table 1. The QCT result is significantly smaller than the value of 44% predicted by a hard sphere model assuming isotropic scattering [*Libby,* 1947], which was used by *Logan and McElroy* [1977] in a study of energetic O atoms and *Solomon* [1983] in an estimate of the significance of fast N atoms on odd nitrogen chemistry. Although the final translational energy distribution function illustrated in Figure 1 could be used directly in the kinetic model, a simpler approach is to estimate an effective relaxation cross section based on the total cross section and average translational energy transferred per collision.

The effective relaxation cross section can be calculated by first estimating the average number of collisions necessary to relax atoms of initial energy E_T to an average final energy corresponding to a translational temperature of 500 K. This is done by using the average fraction of translational energy transferred during a N+N_2 collision, listed in Table 1, as a function of energy. Since the transfer of translational energy is rather inefficient (approximately 5% as shown in Table 1), as many as 70 collisions are necessary to relax a 3 eV N(^4S) atom to a final energy of ~ 0.06 eV, a collisional efficiency similar to vibrational relaxation. The thermalization cross section is then estimated as the total cross section per collision. The energy dependence of these estimated cross sections, which are a factor of 5–25 smaller than the gas kinetic value of 3.5×10^{-15} cm^2 and are now comparable to the N(^4S)+O_2 reaction cross section [*Duff et al.,* 1994], are given in Table 1. The influence of the significantly smaller relaxation cross sections on the formation of NO is discussed in section 3.

The possible enhancement of NO removal rate by fast N(^4S) atoms deserves some comment. It is generally accepted that the N+NO reaction rate in the temperature range of 196-3152 K is temperature independent with a value of 3.4×10^{-11} cm^3 s^{-1} [*Lee et al.,* 1978; *Michael and Lim,* 1992]. These measurements almost certainly indicate that in this temperature range the reaction occurs on the ground state potential energy surface (PES) with little or no barrier. However, it has been shown that for the N+NO reaction there exists

Table 1. Relaxation Cross Sections for Fast N(^4S) Atoms

E_T, eV	σ_{in}, 10^{-16} cm^2	σ_{el}, 10^{-16} cm^2	$< \Delta f_T >$	N_{col}	σ_{eff} 10^{-16} cm^2
0.075	14.6	203.9	0.059	2	109.3
0.125	19.2	178.1	0.058	11	17.9
0.25	23.5	148.3	0.056	23	7.4
0.50	25.2	124.3	0.054	35	4.3
0.75	25.8	112.1	0.052	43	3.2
1.0	25.7	104.5	0.051	48	2.7
1.5	25.3	94.7	0.048	56	2.1
2.0	24.7	88.6	0.046	62	1.8
2.5	24.5	83.9	0.044	67	1.6
3.0	24.1	80.4	0.042	70	1.5

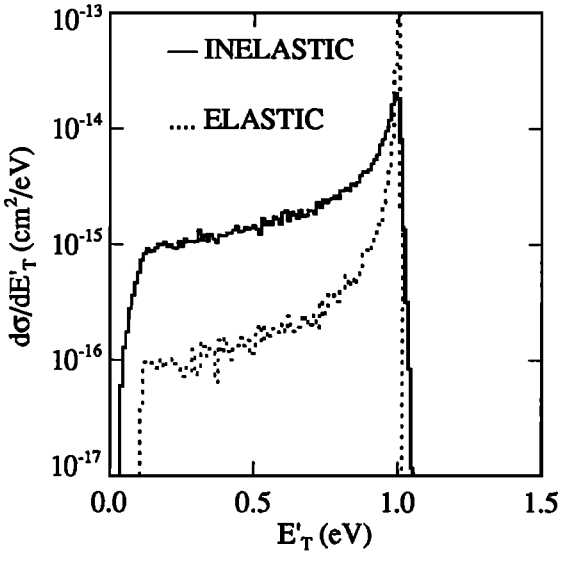

Figure 1. Inelastic (solid line) and elastic (dashed line) components of the differential translation energy transfer cross section at an initial translation energy of 1 eV.

an excited state PES with a barrier of approximately 0.6 eV [*Walch and Jaffe,* 1987]. Although not important for thermal rate constants, this excited state PES could make a significant contribution to the energy dependent rate constant needed for the nonthermal translational energy encountered in the present work. Work in progress (J. W. Duff and R. D. Sharma, manuscript in preparation, 1996) indicates an increase of approximately 20% in energy-independent N+NO reaction rate constant of 3.4×10^{-11} cm^3 s^{-1} at a N(^4S) translational energy of 1 eV increasing to approximately a factor of 2 at an energy of 1.5 eV. The importance of nonthermal effects in the N+NO reaction on NO production can be estimated by considering the N(^4S) EDF (see Figure 3) at 110 km. The most important effect of the increased N+NO reaction rate due to nonthermal effects and excited state PES occurs for energies greater than 1 eV, where less than 50% of the NO production from N(^4S) occurs. Thus an increase of up to a factor of 2 at energies greater than 1 eV would at most decrease the total NO number density by 25% at 110 km where the N(^2D)+O_2 reaction is also a source of NO. As altitude increases, the effect of fast N+NO collisions becomes less important. A more quantitative estimate of the importance of nonthermal effects due to the N+NO reaction requires using the energy dependent N+NO reaction rate constant directly in the calculation of the N(^4S) distribution.

3. Results and Discussion

All the calculations are made for the equatorial lower thermosphere, low ($F_{10.7} = 71$) and high ($F_{10.7} = 245$) solar activity conditions and quiet geomagnetic conditions. The major constituent and temperature vertical distribution are provided by the MSIS-86 model [*Hedin,* 1987]. The extreme ultraviolet solar irradiances are taken from *Tobiska* [1991] ajusted to the adequate $F_{10.7}$ value. In addition to the solar EUV flux, we include a soft X ray component from 18 to 50 Å. It is taken from the solar reference spectrum for solar minimum conditions labeled SC21REFW [*Hinteregger et al.,* 1981]. Using the baseline solar minimum reference spectrum, we scale the dependence on solar activity conditions on the basis of the integral energy fluxes for this wavelength interval provided by Tobiska's model. The soft X ray flux is further extended down to 11 Å by using *Donnelly and Pope*'s [1973] data. The spectrum in the interval 11–17 Å was only measured for moderate solar activity ($F_{10.7}$=143). For different solar activity levels, we scale these values linearly with the $F_{10.7}$ index. We also conduct some additional runs illustrating the model sensitivity to poorly defined model parameters such as elastic cross sections and the value of the solar soft X ray flux.

As mentioned before, at the first step of the model calculation, we evaluate the frequencies of solar EUV, XUV, and soft X ray and photoelectron interaction with the ambient atmospheric gas. Figure 2 illustrates the relative importance of different processes for the high solar activity case. Curves A, B, and C correspond to the ratio of the photoelectron efficiency ratio $P = Pe/Pi$ where Pi is the photoionization rate due to direct photon interaction and Pe is the photoelectron contribution.

As a check of the validity of our photionization model, these results may be compared with previous work on the effect of secondary ionization by photoelectrons. *Torr and Torr* [1979] found that photoelectron impact ionization increased the ionization rate by ~ 30% between 150 and 250 km. *Richards and Torr* [1988] gave

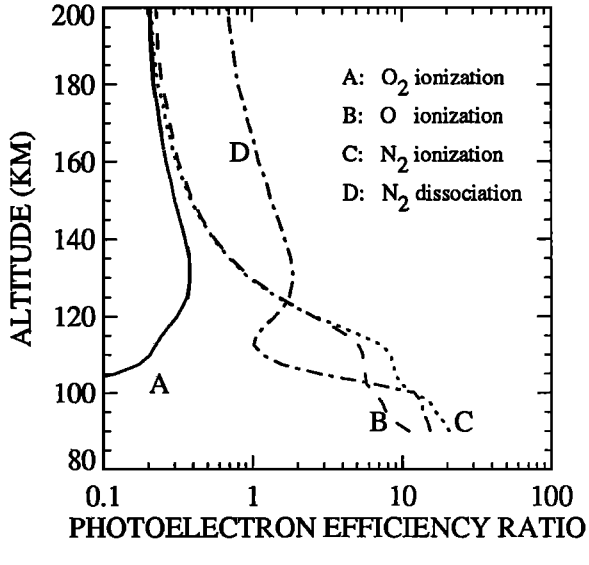

Figure 2. Photoelectron efficiency ratio $R = Pi/Pe$ for different processes. Curve A indicates: O_2 ionization; curve B indicates O ionization; curve C indicates N_2 ionization, and curve D indicates N_2 dissociation. These values are calculated for a high solar activity ($F_{10.7} = 243$) and overhead Sun.

an expression for R for O^+ and N_2^+ with a value of 2.5 at 120 km. Calculations by *Buonsanto et al.* [1992] for winter conditions at Millstone Hill give $R \simeq 8$ for N_2^+ at 100 km. The sensitivity of this ratio to the ionization cross sections and EUV solar flux was recently discussed in detail by *Titheridge* [1996] and compared to earlier calculations. Our results in Figure 2 show the same altitude dependence with slightly larger values below 120 km because of the higher solar activity and smaller solar zenith angle than in Titheridge's calculations. Another important quantity for the N-NO photochemistry is the total dissociation rate of N_2. Figure 2 illustrates that, as for ionization of N_2 and O, secondary photoelectrons substantially increase the production rate of nitrogen atoms. The dip near 110 km corresponds to the altitude of maximum photodissociation efficiency by the solar CIII (977 Å) line [see *Gérard et al.*, 1993, Figure 1a]. This process has no counterpart in N_2 ionization for which the ratio R decreases steadily with altitude. It is seen that at altitudes below 130 km, the role of the high-energy photoelectron becomes dominant. At lower altitudes, the relative influence of electrons generated by soft X ray ionization increases, which leads to an increase of the photoelectron efficiency ratios, especially for N_2.

The relaxation of the initial energy distribution function of hot $N(^4S)$ produced by N_2 dissociation and dissociative ionization by photon and photoelectron fluxes (calculated at step a) and due to exothermic chemical reactions (3) (calculated at step b) was studied in the kinetic model. The calculated steady state energy distribution functions are presented in Figure 3 (solid curves) for 110 and 140 km (curves A and B, respectively) and compared with the local Maxwellian distribution functions (dashed curves). The results are presented for low solar activity in Figure 3a and are presented for high solar activity in Figure 3b. The peaks in the nonthermal curves are physically significant as they are formed by EUV photon absorption and chemical sources of hot particles. The broadening of the initial energy distributions of hot $N(^4S)$ formed in chemical reactions leads to some additional smoothing of the steady state function in the range of chemical reaction energy release. Figure 3 shows that the steady state energy distribution functions of hot $N(^4S)$ remain in nonequilibrium at all altitudes for both levels of solar activity. There are indications that the nonthermal fraction of the energy distribution functions can influence the characteristics of the NO IR emission spectra [*Sharma et al.*, 1993; *Armstrong et al.*, 1994].

The fraction of hot $N(^4S)$ reacting with O_2, that is, the reaction efficiency may be calculated using the steady state EDF. This quantity strongly depends on the values of the reaction cross sections and the energy dependent cross sections in elastic and inelastic collisions of hot $N(^4S)$ with the atmospheric constituents. The energy dependent cross section for reaction of hot $N(^4S)$ with O_2 was calculated by different groups [*Polak et al.*, 1984; *Duff et al.*, 1994] and is in a good agreement. Therefore we adopt Polak et al.'s curve in our

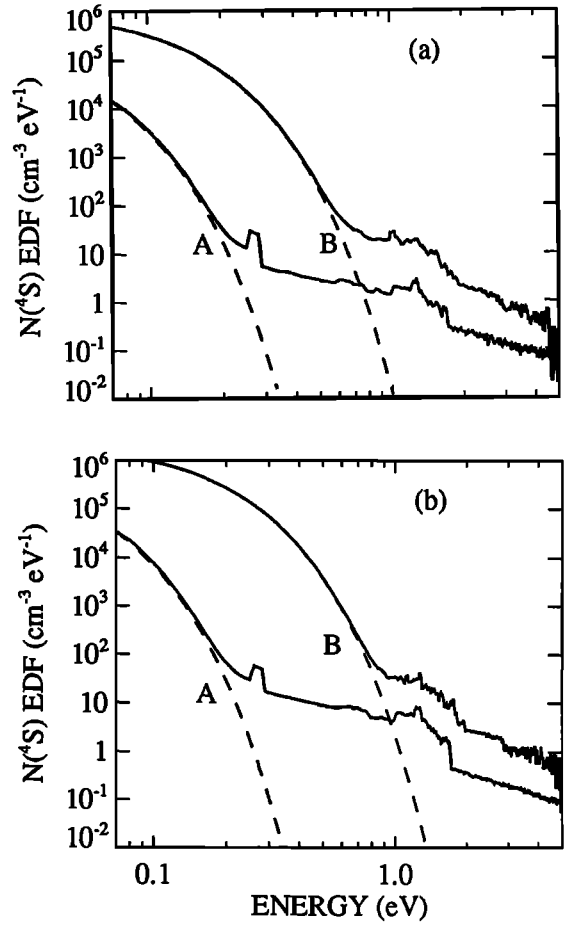

Figure 3. Steady state energy distribution function of $N(^4S)$ at 110 km (curve A) and 140 km (curve B). Solid lines show the calculated energy distribution function (EDF), and dashed curves are the local Maxwellian EDFs for gas temperatures of 209 K (curve A) and 575 K (curve B). (a) Low solar activity case ($F_{10.7} = 71$). (b) High solar activity case ($F_{10.7} = 245$)

model, and we assume that it is known with sufficient accuracy. Measurements of the energy dependence of the elastic cross sections of hot $N(^4S)$ are not available for O_2 and O. In our previous studies, we used the model of energy independent hard spheres with values deduced from the consideration of diffusive processes [*Morgan and Schiff*, 1964]. The height profile of the reaction efficiency for this case is presented in Figure 4. In this study, we use the energy dependent effective cross section for collisional relaxation of hot $N(^4S)$ with N_2 described in section 2.3. The reaction efficiency for the case when the elastic cross sections have hard sphere values and the N-N_2 collisions are taken from Table 1 is presented in Figure 4 as well. To evaluate the sensitivity of the model to the relaxation cross sections, we also calculate the reaction efficiency when all elastic cross sections are energy dependent in the same manner as calculated for N-N_2 collisions. It is seen that the consideration of the energy dependence of the relaxation cross sections leads to a significant increasing of the reaction efficiency and hence to an enhanced hot

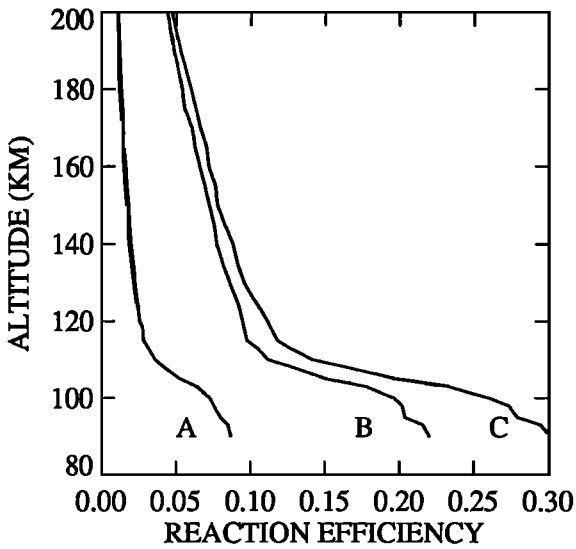

Figure 4. Altitude dependence of the $N_f(^4S)+O_2$ reaction efficiency for high solar activity and different models of elastic cross sections: curve A, hard sphere approximation ($\sigma_{el} = 10^{-15}$ cm^2), curve B, hard sphere approximation for $N_f(^4S)+O_2$ collisions and energy dependent cross section for $N_f(^4S)$ + N_2, and curve C, energy dependent cross section for collision of $N_f(^4S)$ with O_2, O, and N_2.

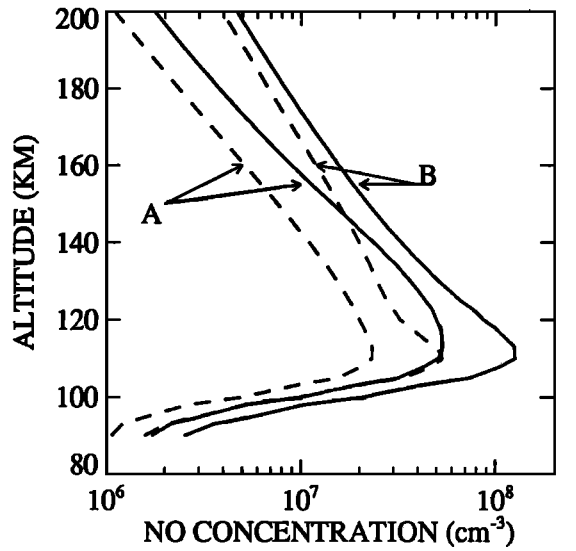

Figure 5. Nitric oxide density profiles for low (curves A) and high (curves B) solar activity levels. Dashed lines show the values for the standard NO photochemistry (no fast N); solid lines are for the hot N cases.

$N(^4S)$ effect on the odd nitrogen photochemistry. The altitude profile of the reaction efficiency only weakly depends on the level of solar activity. Therefore only the case of high solar activity is presented here.

Using the distribution of hot $N(^4S)$ described before, we calculate the influence of these nonthermal N atoms on the nitric oxide density in the lower thermosphere. The results of these calculations are presented in Figure 5 for low and high solar activity conditions. The dashed curves correspond to the standard cases, and the solid curves correspond to hot N cases. The revisions of the photochemical model lead to an increase of the the NO densities in comparison with our previous studies [*Gérard et al.*, 1993, 1995]. The presence of hot $N(^4S)$ also leads to a very significant increase of the NO densities. The hot N cases shown in Figure 5 are calculated for the case when the elastic cross sections of the hot $N(^4S)$-N_2, O_2, and O collisions include the energy dependence from Table 1. This run corresponds to larger values of the reaction efficiency,that is to curve C in Figure 4. The NO peak densities for the curves presented in Figure 5 are also listed in Table 2.

The results given in Table 2 show that the inclusion into the model of the soft X ray flux extension down to 11 Å, and the Auger and dissociative ionization lead to an increase of the standard case NO peak densities up to 36% for maximum solar activity. The main reason for the higher NO densities is the increase of the N_2 ionization rate due to production of more energetic photoelectrons in the lower thermosphere. The addition of hot $N(^4S)$ into the model leads to a significant additional increase of the NO densities. For both low and high solar activities, this effect gives a more than twofold increase in comparison with the standard case.

A few additional runs have been conducted to check the sensitivity of the model to different uncertain parameters. To assess the influence of the elastic cross sections, we calculate the NO height profiles for high solar activity for the three different cross-sections approaches described before. We find that the NO peak density increases by 29% in comparison with the standard case for the simplest case of the hard sphere approximation. For the intermediate case, the increase is 92% and 136% for the energy dependent relaxation cross section. It is likely that the latter case is more justified as the existence of an elastic cross section energy dependence for N-N_2 collisions is based on physical arguments developed before. The consideration of the energy dependence of the N-O_2 relaxation cross sections, not presently available, will improve the model, but it is clear that it will not significantly modify the values of the calculated NO increase, but it will remain between 92% and 136%.

We also investigate the sensitivity of the model to the value of the XUV and soft X ray solar fluxes. As

Table 2. Calculated Nitric Oxide Peak Density

Solar Activity	Previous Standard*	Standard	Hot N
Solmin	1.3(7)	2.3(7)	5.4(7)
Solmax	3.9(7)	5.3(7)	1.3(8)

Note that 1.3 (7) should read 1.3×10^7. Units are per cubic centimeter.

*See *Gérard et al.* [1993].

mentioned before, previous runs use the values of these fluxes derived from observations. There are indications that the soft X ray flux may exhibit larger variations with solar activity than *Tobiska*'s[1991] values [*Siskind et al.,* 1995]. Therefore we conducted a run using the same scaling factor of the soft X ray flux as used by *Siskind et al.* [1995] to fit the calculated NO densities to the high values of nitric oxide obtained in microwave measurements by *Clancy et al.* [1992]. For the interval 18–50 Å, we increase the baseline values of SC21REFW by a scaling factor of 100, and in interval 11–17 Å, the measured value was increased by a factor 75. The NO density profiles for the standard case and for the case with hot $N(^4S)$ contribution are presented in Figure 6. For the standard case, the NO peak density is about 1.5×10^8 cm^{-3}, and for the hot N case, the NO peak density about 4.0×10^8 cm^{-3}.

4. Summary

The production and steady state density of thermospheric nitric oxide have been reexamined after revision and updates of the photochemical and hot N kinetic models. The soft X ray solar flux has been extended down to 11 Å. In addition to the direct increase, Auger photoelectons produced with high energy contribute to further ionization and dissociation of N_2 which subsequently produce NO. The photoelectron efficiency ratio indicates that fast electrons play a dominant role in the dissociation and ionization of N_2 in the lower thermosphere in agreement with the conclusions of other recent studies. These photochemical updates to the model based on the work by *Siskind et al.* [1995] produce an increase in the calculated NO density in comparison with our earlier version.

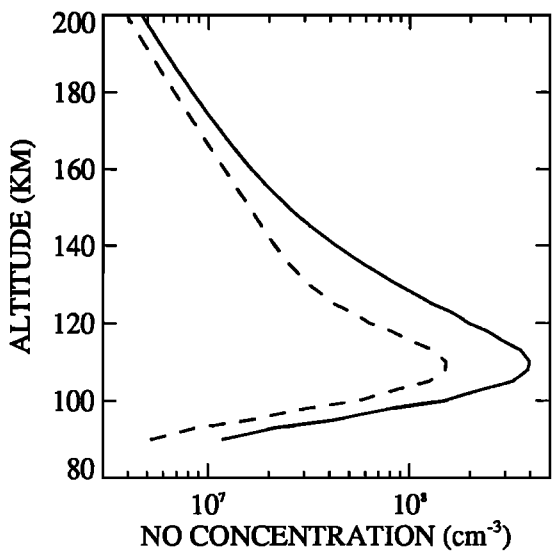

Figure 6. Nitric oxide density profiles for high solar activity conditions using the scaled version of the soft X ray solar flux. Dashed line is for the standard NO chemistry; solid line is for the hot N case.

Significant improvements to the hot N kinetic calculation also produce a substantial increase in the NO production by collisions of $N_f(^4S)$ with O_2. The initial energy distribution of the nonthermal $N(^4S)$ atoms created by exothermic processes have been calculated using a Monte Carlo code. In addition, hot N production by N_2 dissociative ionization has been considered. Even more importantly, a new calculation indicates that the relaxation cross section of $N_f(^4S)$ with N_2 is strongly energy dependent. At nonthermal energies, it is substantially smaller than the hard sphere approximation value previously used, and, consequently, the $N(^4S)$ distribution function has a larger high-energy component than previously thought. These changes to the $N_f(^4S)$ model produce an additional twofold increase in the NO peak density. If scaling factors larger than those in *Tobiska's* [1991] solar flux model are applied, NO densities as high as 4×10^8 cm^{-3} are reached. Since such values exceed the observed NO densities. However, it must be kept in mind that the values calculated here are for equatorial steady state conditions. They must be considered as upper limits in comparison to the actual densities which undergo a diurnal variation. These results, nevertheless, indicate that the N atoms are a major source of thermospheric nitric oxide.

Acknowledgments. We thank R. Locht for valuable discussions and B. Van Zyl and J. Ajello for communicating laboratory results before publication. J.-C. Gérard is supported by the National Fund for Scientific Research (FNRS). J. W. Duff acknowledges support from the Internal Research and Development program at Spectral Sciences, Inc. This research was partly funded by FRFC grant 2.4539.93 and by the Russian Foundation for Fundamental Research (RFFR grant 96-02-16389).

The Editor thanks D.W. Rusch and D.E. Siskind for their assistance in evaluating this paper.

References

Armstrong, P.S., S.J. Lipson, J.A. Dodd, J.R. Lowell, W.A. M. Blumberg, and R.M. Nadile, Highly rotationally excited NO (v,J) in the thermosphere from CIRRIS 1A limb radiance measurements, *Geophys. Res. Lett., 21,* 2425, 1994.

Barth, C.A., W.K. Tobiska, D.E. Siskind, and D.D. Cleary, Solar–terrestrial coupling: Low–latitude thermospheric nitric oxide, *Geophys. Res. Lett., 15,* 92, 1988.

Barth, C.A., C.B. Farmer, D.E. Siskind, and J.P. Perich, ATMOS observations of nitric oxide in the thermosphere and lower mesosphere, *J. Geophys. Res., 101,* 12,489, 1996.

Bernstein, R. B., A. Dalgarno, H. Massey, and I. C. Percival, Thermal scattering of atoms by homonuclear diatomic molecules, *Proc. R. Soc. London A, 274,* 427-442, 1963.

Buonsanto, M.J., S.C. Solomon, and W.K. Tobiska, Comparison of measured and modeled solar EUV flux and its effect on the $E - F1$ region ionosphere, *J. Geophys. Res., 97,* 10,513, 1992.

Clancy, R. I., D. W. Rusch, and D. O. Muhleman, A microwave measurement of high levels of thermospheric nitric oxide, *Geophys. Res. Lett., 19,* 261, 1992.

Conway, R.A., Photoabsorption and photoionization cross section of O, O_2 and N_2 for photoelectron production calculations: A compilation of recent laboratory measure-

ments, *Rep. 6155*, Nav. Res. Lab., Washington, D.C., 1989.

Donnelly, R.F., and J.H. Pope, The 1–3000 Å solar flux for a moderate level of solar activity for use in modeling the ionosphere and upper atmosphere, *Tech. Rep. ERL 276*, Natl. Oceanic and Atmos. Admin., Silver Spring, Md., 1973.

Duff, J.W., F. Bien, and D.E. Paulsen, Classical dynamics of the $N(^4S)+O_2(X\,^3\Sigma_g) \rightarrow NO(X\,^2\Pi)+O(^3P)$ reaction, *Geophys. Res. Lett.*, 21, 2043, 1994.

Eparvier, F.J., and C.A. Barth, Self absorption theory applied to rocket measurements of the nitric oxide (1, 0) γ band in the daytime thermosphere, *J. Geophys. Res., 97*, 13,723, 1992.

Fell, C. , J.I. Steinfeld, and S. Miller, Quenching of $N(^2D)$ by $O(^3P)$, *J. Chem. Phys., 92*, 4768, 1990.

Gardner, J.L., and J.A.R. Samson, Photoion and photoelectron spectroscopy of CO and N_2, *J. Chem. Phys., 62*, 1447, 1975.

Gérard, J.-C., and C. Taieb, The *E*-region electron density diurnal asymmetry at Saint-Santin: Observations and role of nitric oxide, *J. Atmos. Terr. Phys., 48*, 471, 1986.

Gérard, J.C., V.I. Shematovich, and D.V. Bisikalo, Nonthermal nitrogen atoms in the Earth's thermosphere, 2, A source of nitric oxide, *Geophys. Res. Lett., 18*, 1695, 1991.

Gérard, J.C., V.I. Shematovich, and D.V. Bisikalo, Effect of hot $N(^4S)$ atoms on the NO solar cycle variation in the lower thermosphere, *J. Geophys. Res., 98*, 11,581, 1993.

Gérard, J.C., V.I. Shematovich, and D.V. Bisikalo, The role of fast $N(^4S)$ atoms and energetic photoelectrons on the distribution of NO in the thermosphere, in *The Upper Mesosphere and Lower Thermosphere: A review of experiment and theory, Geophys. Monogr. Ser.*, vol. 87, 235, AGU, Washington, D.C., 1995.

Hedin, A., MSIS-86 thermospheric model, *J. Geophys. Res., 92*, 4649, 1987.

Hinteregger, H.E., K. Fukui, and B.R. Gibson, Observational reference and model data on solar EUV from measurements on AE-E, *Geophys. Res. Lett., 8*, 1147, 1981

Hirschfelder, J.O., C.F. Curtiss, and R. B. Bird, *Molecular Theory of Gases and Liquids*, 1219 pp., John Wiley, New York, 1954.

LaBudde, R.A., and R.B. Bernstein, Classical study of rotational excitation of a rigid rotor: Li^++H2, II, Correspondence with quantal results, *J. Chem. Phys., 59*,3687, 1973.

Laganà, A., E. Garcia, and L. Ciccarelli, Deactivation of vibrationally excited nitrogen molecules by collision with nitrogen atoms, *J. Phys. Chem., 91*, 312-314, 1987.

Lee, J.H., J.V. Michael, W.A. Payne, and L.J. Stief, Absolute rate of the reaction of $N(^4S)$ with NO form 196-400 K with DF-RF techniques, *J. Chem. Phys. 69*, 3069, 1978.

Libby, W.F., Chemistry of energetic atoms produced by nuclear reactions, *J. Am. Chem. Soc., 69*,2523, 1947.

Locht, R., W. Denzer, E. Rühl, and H. Baumgärtel, Photoionization mass spectrometry of kinetic energy-selected ions: The translational energy distribution of N^+/N_2 in the inner-shell ionization energy range, *Chem. Phys., 160*, 477, 1992.

Logan, J.A. and M.B. McElroy, Distribution functions for energetic oxygen atoms in the Earth's lower atmosphere, *Planet. Space Sci., 25*, 117-122, 1977.

Massey, H.S.W., and C.B.O. Mohr, Free paths and transport phenomena in gases and the quantum theory of collisions, II, The determination of the laws of force between atoms and molecules, *Proc. R. Soc. London A, 144*, 188-205, 1934.

Michael, J.V., and K.P. Lim, Rate constants for the N_2O reaction system: Thermal decomposition of N_2O; N + NO $\rightarrow$ N_2 + O; and implications for O + N_2 $\rightarrow$ NO + O, *J. Chem. Phys., 97*, 3228, 1992.

Moddeman, W.E., T.A. Carlson, M.O. Krause, B.P. Pullen, W.E. Bull, and G.K. Schweitzer, Determination of the K-LL Auger spectra of N_2, O_2, CO, NO, H_2O, and CO_2, *Chem. Phys., 55*, 2317, 1971.

Morgan, J.E., and H.J Schiff, Diffusion coefficients of O and N atoms in inert gases, *Can. J. Phys., 47*, 300, 1964.

Pattengill, M.D., A comparison of classical trajectory and exact quantal cross sections for rotationally inelastic Ar-N2 collisions, *Chem. Phys. Lett., 36*, 25-28, 1975.

Polak, L.S., M.Y. Goldenberg, and A.A. Levitsky, *Computational Methods in Chemical Kinetics*, Nauka, Moscow, 1984.

Rees, M.H., *Physics and chemistry of the upper atmosphere*, Cambridge Univ. Press, New York, 1989.

Richards, P.G., and D.G. Torr, Ratios of photoelectron to EUV ionization rates for aeronomic studies, *J. Geophys. Res., 93*, 4060, 1988.

Richards, P.G., J.A. Fennelly, and D.G. Torr, EUVAC: A solar EUV flux model for aeronomic calculations, *J. Geophys. Res., 99*, 8981, 1994

Sharma, R.D., Y. Sun, and A. Dalgarno, Highly rotationaly excited nitric oxide in the terrestrial thermosphere, *Geophys. Res. Lett., 20*, 2043, 1993

Sharma, R.D., V.A. Kharchenko, Y. Sun, and A. Dalgarno, Energy distribution of fast nitrogen atoms in the nighttime terrestrial thermosphere, *J. Geophys. Res., 101*, 275, 1996.

Shematovich, V.I., D.V. Bisikalo, and J.C. Gérard, Non thermal nitrogen atoms in the Earth's thermosphere, 1, Kinetics of hot $N(^4S)$, *Geophys. Res. Lett., 18*, 1691, 1991.

Shematovich, V.I., D.V. Bisikalo, and J.C. Gérard, The thermospheric odd nitrogen photochemistry: Role of nonthermal $N(^4S)$ atoms, *Ann. Geophys., 10*, 792, 1992.

Siskind, D.E., C.A. Barth, and D.D. Cleary, The possible effect of solar soft X rays on thermospheric nitric oxide, *J. Geophys. Res., 95*, 4311, 1990.

Siskind, D.E., D.J. Strickland, R.R. Meier, T. Majeed, and F.G. Eparvier, On the relationship between the solar soft X ray flux and thermospheric nitric oxide: An update with an improved photoelectron model, *J. Geophys. Res., 100*, 19,687, 1995.

Solomon, S., The possible effects of translationally excited nitrogen atoms on lower thermospheric odd nitrogen, *Planet. Space Sci., 31*, 135, 1983.

Tharamel, J., V. Kharchenko, and A. Dalgarno, Thermalization of fast atoms in an oxygen atmosphere: Quantum calculations of energy transition rates in elastic collisions (abstract), *Eos Trans. AGU, 76 (46)*,Fall Meet. Suppl. F438, 1995.

Titheridge, J.E., Direct allowance for the effect of photoelectrons in ionospheric modeling, *J. Geophys. Res., 101*, 357, 1996.

Tobiska, W.K., Revised solar extreme ultraviolet flux model, *J. Atmos. Terr. Phys., 53*, 1005, 1991.

Torr, D.G., and M.R. Torr, Chemistry of the thermosphere and ionosphere, *J. Atmos. Terr. Phys., 41*, 797, 1979.

Truhlar, D.G., and J.T. Muckerman, Reactive scattering cross sections, III, Quasiclassical and semiclassical methods, in *Atom-Molecule Collision Theory*, edited by R. B. Bernstein, pp. 505-566, Plenum, New York, 1979.

Van Zyl, B., and T.M. Stephen, Dissociative ionization of H_2, N_2, and O_2 by electron impact, *Phys. Rev. A, 50*, 3164, 1994.

Walch, S.P., and R.L. Jaffe, Calculated potential surfaces for the reactions: $O + N_2 \rightarrow NO + O$ and $N + O_2 \rightarrow NO + O$, *J. Chem. Phys., 86,* 6946, 1987.

Whipple, E.G., Jr., Theory of reaction product velocity distributions, *J. Chem. Phys., 60,* 1345, 1974.

Yee, J. H., and A. Dalgarno, Energy transfer of $O(^1S)$ atoms in collision with $O(^3P)$ atoms, *Planet. Space Sci., 33,* 825, 1985.

D. V. Bisikalo and V. I. Shematovich, Institute of Astronomy of the Academy of Sciences, Pyatnistkaya Street, 48, Moscow 109017, Russia. (e-mail: bisikalo@inasan.rssi.ru; shematov@inasan.rssi.ru)

J.W. Duff, Spectral Sciences, Inc., 99 S. Bedford, Burlington, MA 01803. (e-mail: duff@spectral.com)

J.-C. Gérard, Laboratoire de Physique Atmosphérique et Planétaire, Institut d'Astrophysique, Université de Liège, 5, avenue de Cointe, B-4000 Liège, Belgium. (e-mail: gerard@astro.ulg.ac.be)

(Received April 12, 1996; revised September 16, 1996; accepted September 16, 1996.)